Thai Journal of Mathematics
Volume 6 (2008) Number 7 : 89–108
www.math.science.cmu.ac.th/thaijournal

The Application of Curvilinear Coordinate for Primitive Equation in the Gulf of Thailand

W. Wannawong, U. Humphries and A. Luadsong

Abstract : The curvilinear grid is mapped onto a place in which the irregular basin is transformed into a series of connected rectangles. An equispaced grid is used in the connected rectangle system, and all the calculations are conveniently performed in this system. The advantage of such a grid is that the boundary of the water body always falls on a coordinate line and the grid points are closely spaced in the narrow and shallow areas. In this paper, we modify the Princeton Oceanic Model (POM) to study the formulations and its applications of the primitive equations that are generated to the orthogonal curvilinear coordinate (OCC) system and used for the horizontal coordinates in a three-dimensional circulation model. The area of the study covers from $98.54°E$ to $105.54°E$ in longitude and $5.54°N$ to $14.54°N$ in latitude. In addition, we also study the pressure gradient error (PGE) tested with both of the OCC grids and orthogonal rectangular coordinate (ORC) grids. The resolution grid points of the OCC and ORC grids have the same number of 37×97 in longitude (E) and latitude (N), respectively. The vertical resolution is 10 vertical levels. The result of the study indicate that the actual flow is produced directly by wind forcing induced the circulation inside the Gulf of Thailand (GoT) characterized by the migration of water from the southeast to the north of the GoT. Using of the OCC system has made possible high resolution required without paying the penalty imposed by unnecessary high resolution in other parts of the region. Furthermore, the comparison of the averaged velocity induced by the PGE between the OCC and ORC grids with the same number of grid points show that the OCC grids are more efficient for the GoT than the rectangular grids. The OCC grids are very useful for description about the circulation in the coastal ocean modeling, especially a coastal region in the GoT with complex coastlines and the steepness of topography.

Keywords : Curvilinear coordinate, Gulf of Thailand, Pressure gradient error, Primitive equations.

2000 Mathematics Subject Classification : 81T80, 91B76, 91B74.

1 Introduction

Thailand may be divided into five major physical regions: the central valley, the continental highlands of the north and northwest, the northeast, the southeast coast, and the peninsula. The heartland of the nation is the central valley, fronting the Gulf of Thailand (GoT) and enclosed on three sides by hills and mountains. The small southeast coast region faces the GoT and is separated from the central valley and Cambodia by hills and mountains that rise in places to over 1,500 m (5,000 ft). Most of the people live along the narrow coastal plain and the restricted river valleys that drain southward to the Gulf. In the oceanic model, the bending of the Gulf is the important problem to develop the model which has been affected by the prediction; the sea surface elevation, the wave speed and direction of the velocity of water flowing in the GoT, the temperature as well as the salinity in the shoreline. The physical domain of the GoT that is the irregular grid has the lateral boundary which is complex and complicate. In this paper, we study the orthogonal curvilinear coordinates (OCC) system which is the interesting technique for solving the irregular shape of the GoT. A three-dimensional time-dependent numerical Princeton Oceanic model (POM) using the OCC is presented. The OCC system is based on a conformal mapping of the interior region bounded by the actual coast, the seaward boundary and two parallel lateral boundaries into a rectangle in the image plane. Since the transformation is conformal, the associated modifications of the vertically integrated equations of motion and mass continuity are minimized. The coast, seaward boundary, and the lateral boundaries of the computing grid are straight lines in the image plane thus facilitating the application of the boundary conditions. The tradition in estuarine, lake and ocean circulation modeling has been used to finite difference techniques on a rectangular gird. There are many instances however, when the computational resources required to do so become excessive. This situation arises in regions where the coastline has prominent features or where boundary layer dynamics are important. If the number of points is not large enough resolve the coastal features or boundary layer, then the numerical solution is likely to have errors even in the interior regions. In recent years, a number of programs for generating the OCC grids and prognostic models for using them have been developed. One of the obvious considerations for global ocean modeling has been desired to keep grid singularities away from the ocean domain and avoid the numerical problems that they cause. Grid generation programs that accomplish this have been written by Madec and Imbard (1996), Murray (1996), and Smith *et. al.* (1995). While keeping singularities away from ocean areas remain a desideratum, OCC grids also have the advantage of allowing greater flexibility of grid orientation, alignment, and density. Grids for the limited-area models of Blumberg and Mellor (1987) and Haidvogel *et. al.* (1991) are generated by a program written by Wilkin (1987, unpublished manuscript) and specifically designed to allow at least one boundary to follow a smoothed coastline.

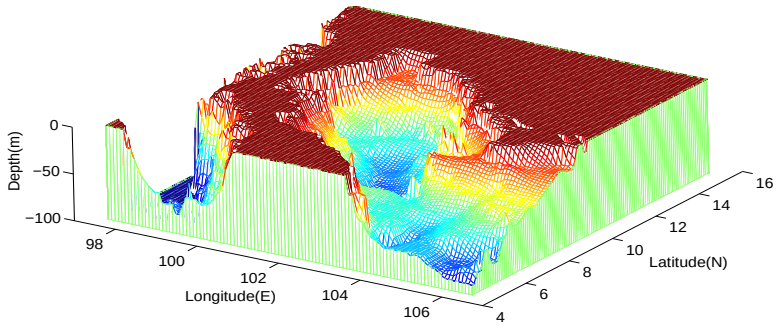

Figure 1: Three dimensional perspective view of the Gulf of Thailand domain.

The purpose of this paper is to study the formulations and its applications of the primitive equations that are generated to the OCC system and used for the horizontal coordinates in a three-dimensional circulation model by modifying the POM2k (version 2004) in the GoT. The area of the study covers from $98.54°E$ to $105.54°E$ in longitude and from $5.54°N$ to $14.54°N$ in latitude which is shown in Figure 1.

2 Model Formulation

2.1 The Governing Equations

The mathematical modeling of this research is based on the primitive equation, which concerns with the basic equations as the continuity, momentum, hydrostatic, temperature, salinity, density and by the assumption of the ocean is incompressible respectively. Two approximations are used; first is hydrostatic assumption, and second is Boussinesq approximation. The rectangular coordinates are the easiest to illustrate the principles of the equation, an advantage in using vector notation. Let (u, v, w) be the fluid velocities in the zonal, meridional and locally vertical direction described by Mellor (2004, Users Guide for a Three-Dimensional, Primitive Equation, Numerical Ocean Model).

The horizontal equations of motion are

$$\frac{du}{dt} = -\frac{1}{\rho_0}\frac{\partial p}{\partial x} + fv + \frac{\partial}{\partial z}(A_{mv}\frac{\partial u}{\partial z}) + F_x, \tag{2.1}$$

$$\frac{dv}{dt} = -\frac{1}{\rho_0}\frac{\partial p}{\partial y} - fu + \frac{\partial}{\partial z}(A_{mv}\frac{\partial v}{\partial z}) + F_y, \tag{2.2}$$

where u and v are the corresponding current components in the horizontal coordinate $(m\ s^{-1})$, t is the time (s), ρ_0 is the reference density of the ocean $(kg$

m^{-3}), the parameter $f = 2\Omega \sin\theta$ is the Coriolis parameter where Ω is the speed of angular rotation of the Earth by $\Omega = 7.2921 \times 10^{-5}\ rad\ s^{-1}$, A_{mv} is the vertical eddy viscosity ($m^2\ s^{-1}$) and the terms F_x and F_y are the horizontal viscosity terms respectively.

The hydrostatic equation:

$$\frac{\partial p}{\partial z} = -\rho g, \tag{2.3}$$

where p is the local pressure (Pa) and g is the magnitude of gravitational acceleration ($m\ s^{-2}$).

The continuity equation:

$$\frac{\partial w}{\partial z} + \frac{\partial u}{\partial x} + \frac{\partial v}{\partial y} = 0, \tag{2.4}$$

where w is the velocity in the vertically upward ($m\ s^{-1}$).

The temperature equation:

$$\frac{dT}{dt} = \frac{\partial}{\partial z}(A_{hv}\frac{\partial T}{\partial z}) + F_T, \tag{2.5}$$

where T is the potential temperature (°C).

The salinity equation:

$$\frac{dS}{dt} = \frac{\partial}{\partial z}(A_{hv}\frac{\partial S}{\partial z}) + F_S, \tag{2.6}$$

where S is the potential salinity (psu), A_{hv} is the coefficient of the vertical eddy diffusivity ($m^2\ s^{-1}$) and the terms F_T and F_S are is the horizontal diffusion terms of temperature and salinity.

The state equation of sea water:

$$\rho = \rho(T, S, z), \tag{2.7}$$

where ρ is the density of sea water ($kg\ m^{-3}$) given by Unesco (1981).

The terms F_x, F_y, F_T and F_S found in Equations (1), (2), (5), and (6) represent these unresolved processes and in analogy to molecular diffusion can be written as

$$\begin{aligned} F_x &= \frac{\partial}{\partial x}\Big[2A_m\frac{\partial u}{\partial x}\Big] + \frac{\partial}{\partial y}\Big[A_m\Big(\frac{\partial u}{\partial y} + \frac{\partial v}{\partial x}\Big)\Big], \\ F_y &= \frac{\partial}{\partial y}\Big[2A_m\frac{\partial v}{\partial y}\Big] + \frac{\partial}{\partial x}\Big[A_m\Big(\frac{\partial u}{\partial y} + \frac{\partial v}{\partial x}\Big)\Big], \end{aligned}$$

and

$$F_{T,S} = \frac{\partial}{\partial x}A_H\frac{\partial(T,S)}{\partial x} + \frac{\partial}{\partial y}A_H\frac{\partial(T,S)}{\partial y}.$$

where A_m is the vertical eddy viscosity ($m^2\ s^{-1}$) and A_H is the horizontal mixing coefficient ($m^2\ s^{-1}$).

One should note that F_x and F_y are invariant to coordinate rotation. While, these horizontal diffusive terms are meant to parameterize sub-grid scale processes, in practice the horizontal diffusivities, A_m and A_H, are usually required to damp small-scale computational noise. The form of F_x, F_y and $F_{T,S}$ allows for variable A_m and A_H but thus far they have been held constant. The diffusivities are chosen so that they do not produce excessive smoothing of real features. Values as low as 10 ($m^2\ s^{-1}$) have been used successfully in various applications. The relatively fine vertical resolution used in the applications resulted in a reduced need for horizontal diffusion because horizontal advection followed by vertical mixing effectively acts like horizontal diffusion in a real physical sense. An enhancement, now in progress, is to relate A_m and A_H to the scales of motion begin resolved in the model and to the local deformation field as suggested by Smagorinsky (1963).

The vertical mixing coefficients, A_{mv} and A_{hv}, are obtained by appealing to a second order turbulence closure scheme. The details of the primitive equations and the method of solution have been given by Cox (1984). Finally, the equations are solved for u, v, w, T, S, ρ and p variables by using the leap-frog finite difference technique to explain the circulation in the oceanic model (POM2k) for GoT.

2.2 Numerical Techniques

In the ORC of the POM2k, we use the assumption of fluid which is incompressible with the approximation methods to drive the model (i.e. Thin-shell, Hydrostatic and Boussinesq approximations).

The sigma coordinate (pressure coordinate) is a function of density where the density is a function of temperature and salinity. In order to separate water in the GoT in several layers, the vertical sigma coordinate is used. The model first transforms the equations from z - coordinate (x, y, z, t) into the vertical sigma coordinate (x^*, y^*, σ, t^*) with the relationships:

$$x^* = x, \quad y^* = y, \quad \sigma = \frac{z - \eta}{H + \eta} \quad \text{and} \quad t^* = t$$

where $H(x, y)$ is the bottom topography (m), η is the sea surface elevation (m) and σ is the vertical level ranging from $\sigma = 0$ at $z = \eta$ to $\sigma = -1$ at $z = -H(x, y)$.

In Equations (1)-(7), There are four thermodynamic variables (i.e. p, ρ, T and S). In order to minimize computational errors, the perturbed variables of the ORC can be defined as:

$$\acute{p} \equiv p - \tilde{p}(x, y, z), \qquad \acute{\rho} \equiv \rho - \tilde{\rho}(x, y, z),$$
$$\acute{T} \equiv T - \tilde{T}(x, y, z), \qquad \acute{S} \equiv S - \tilde{S}(x, y, z),$$

where $\tilde{p}(x, y, z)$, $\tilde{\rho}(x, y, z)$, $\tilde{T}(x, y, z)$ and $\tilde{S}(x, y, z)$ are the standard distributions of pressure, density, temperature and salinity respectively. $\tilde{T}(x, y, z)$ and $\tilde{S}(x, y, z)$

can be determined by using observed data, and then according to

$$\begin{aligned} \frac{\partial \tilde{p}(x,y,z)}{\partial z} &= -\tilde{\rho}(x,y,z)g, \\ \tilde{p}(x,y,0) &= \tilde{p}_{as}(x,y). \end{aligned}$$

We derive the mean density by $\tilde{\rho}(x,y,z) \equiv \rho(x,y,z)$ and pressure by $\tilde{p}(x,y,z) = \tilde{p}_{as}(x,y) + g\int_z^0 \tilde{\rho}(x,y,t)dt$, where $\tilde{p}_{as}(x,y)$ is the sea level air pressure computed, based on the atmospheric data.

In the mode splitting, it is desirable in terms of computer economy to separate out vertically integrated equations (external mode) from the vertical structure equations (internal mode). The horizontal currents are defined as:

$$u = \bar{u} + \acute{u}, \qquad v = \bar{v} + \acute{v}.$$

where $(\bar{u}, \bar{v})$ are the vertically averaged currents in the barotropic dynamics (2D):

$$\bar{u} = \int_{-1}^{0} u d\sigma, \qquad \bar{v} = \int_{-1}^{0} v d\sigma$$

and $(\acute{u}, \acute{v})$ are in the baroclinic dynamics (3D), and have no depth average.

Although a three dimensional model is necessary to examine wind induced currents in the majority of the circulation, the main emphasis is on changes in sea surface elevations, and two dimensional form of the model is derived by vertically integrating the equations and expressing the bottom stress in terms of the depth mean current.

From the governing equations are in the partial differential equations (PDE) form. In the POM2k model, the finite difference method is the interested technique for solving the complicated model and also it use the perturbed thermodynamic variables, sigma coordinate and the staggered C-grid given by Arakawa and Lamb (1997). Worachat *et. al.* (2006) had described the sea surface elevation in the spherical coordinate (POM2k) of the GoT. In this paper, we concentrate on the PDE of rectangular coordinate and OCC in the POM2k which is shown in Figure 2.

The k^{th} box has thickness $\Delta\sigma_k$. The horizontal grid is C-grid. The relative positions of the variables on the staggered grid are shown in Figure 3, where $k = 1, 2, ..., k_\circ$ and $k_\circ$ is the total number of vertical layers.

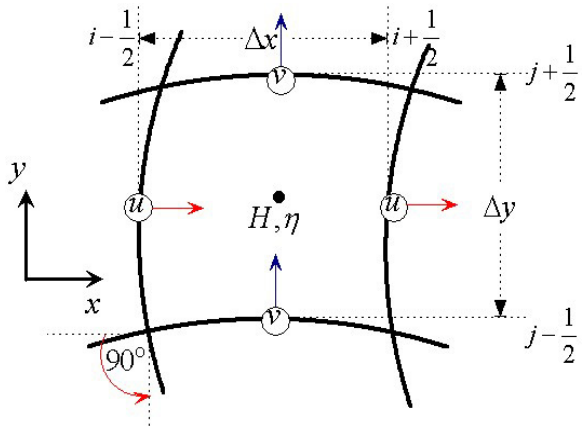

Figure 2: The staggered C–grid of the OCC grid system.

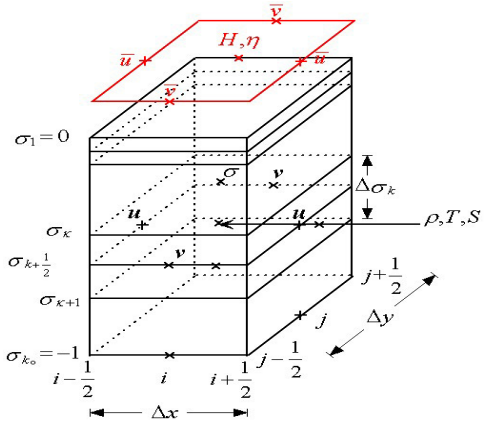

Figure 3: The locations of the variables on the finite difference grid.

The details of the finite difference formulation have been given by Alan *et. al*. (1987). For the model grid, the ORC grids were replaced by the OCC grids to improve coastline representations with 37×97 grid points. In the horizontal coordinate of ORC grids, the average of spacing has ranged 19.25 km and 9.17 km in longitude (E) and latitude (N) respectively. In the horizontal coordinate of OCC grids, the spacing has ranged from 2 to 55 km. The both of coordinates setup the vertical sigma coordinate 10 levels of the three dimensional bathymetry taken from DBDB5 dataset and developed by the U.S. Naval Oceanographic Office (1983, NAVOCEANO) with 1/12 degree longitude-latitude grided resolution and also provided ocean depths every $5^{'}$ of latitude and longitude directions and generated by the conformal mapping. The orthogonal grid generation given by Ives and Zacharias (1987) in Program GRID-DATA of POM which are shown in Figure 4-5, respectively. Aschariyaphotha *et. al*. (2004) has described the techniques that generate the model grid and interpolate the initial data by using the cubic spline and bilinear interpolations. The three dimensional form of the unified equations is simply found by adding the vertical terms, either in σ-coordinates, and reinterpreting the variables as three dimensional quantities. In practical ocean-scale applications, the spherical curvilinear grids combine the advantages of curvilinear grids and of spherical grids. The details of the transformation coordinate system of the primitive equations, represented in Section 2 of Blumberg and Herring (1986).

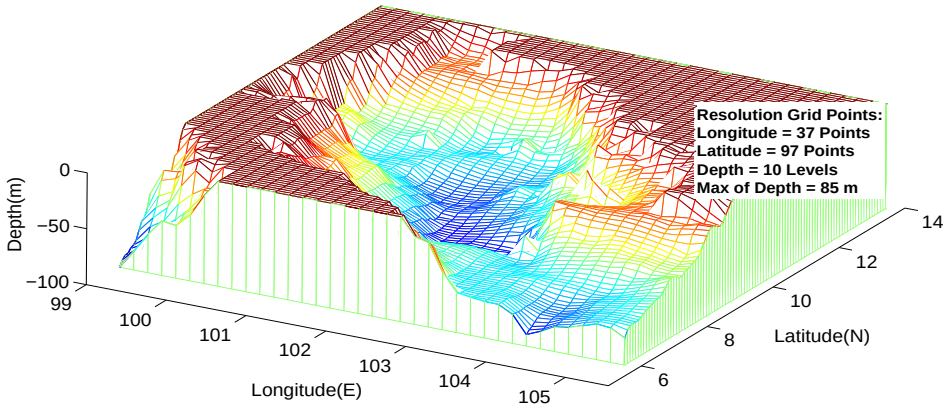

Figure 4: The ORC shown 37×97 grid cells and 10 levels at the closed boundaries with high resolution near the Thailand coast.

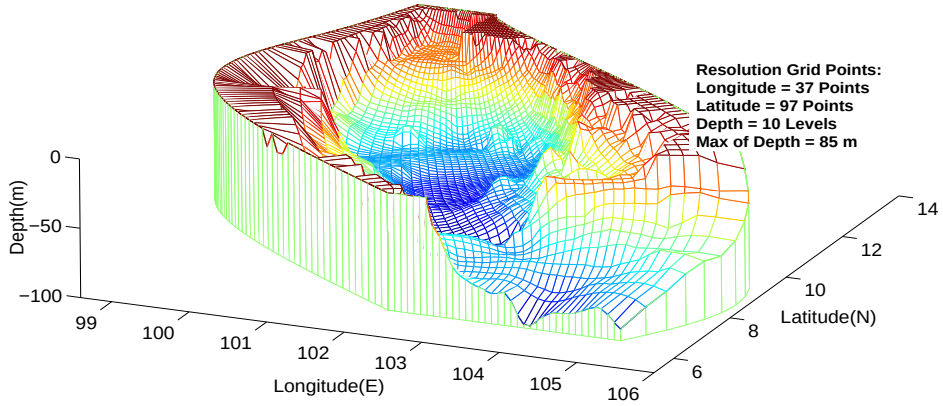

Figure 5: The OCC shown 37×97 grid cells and 10 levels at the closed boundaries with high resolution near the Thailand coast.

3 Model Applications

3.1 Computational Details

To start the model computation, current should be defined at the initial stage. The model starts computation assuming the water velocity is zero everywhere. The model requires initial conditions of wind-stress, temperature, salinity and bottom topography from the observations at each grid points for running the model. We assume that within the condition of the adiabatic process about the closed system of the southern boundary domain. In two dimensional coordinate, the model bathymetry of ORC and OCC are driven from DBDB5 dataset which is shown in Figure 6,11 ; the temperature and salinity fields of ORC are initialized from Levitus94 dataset (1994, Levitus) which is shown from Figure 7 to Figure 9 and OCC is shown from Figure 12 to Figure 14 (i.e. Surface, Middle and Bottom). The resolution of the LEVITUS94 data file is $1^\circ \times 1^\circ$ degree and also generated the climatological monthly mean fields to the model grid in longitude and latitude directions. The wind stress calculated from climatological monthly of mean wind, restoring-type surface heat and salt and climatological monthly of mean freshwater flux taken from the European Centre for Medium-Range Weather Forecasts (1993, ECMWF) with $1.125^\circ \times 1.1213^\circ$ degree longitude-latitude grid resolution and measured at 10 meters above sea surface which is shown in Figure 10a and Figure 15a of ORC and OCC respectively. In this paper, we use the sample case of monthly month in March 1993 (i.e. Temperature and Salinity) and the average of 6-hour wind fields are taken from the period 00UTC on March 1, 1993 to 24UTC on March 31, 1993 to calculate wind stress for the initial data which is shown in Figure 10b and Figure 15b of ORC and OCC respectively. In addition, the horizontal grid spacing has ranged from 2 to 55 km. The west ($99.0^\circ E$) and east ($105.54^\circ E$) boundaries are placed through U-points, whereas south ($5.54^\circ N$) and the north ($13.54^\circ N$) boundaries are through V-points given by Worachat *et. al*. (2006). Let the west, east, north and south boundaries of the model be a rigid wall (i.e. $u_{\frac{1}{2},j} = 0$, $v_{I-\frac{1}{2},j} = 0$, $v_{i,\frac{1}{2}} = 0$ and $v_{i,J-\frac{1}{2}} = 0$). In the ORC and OCC grid models, we approach ideally balances the practical criteria of resolution and accuracy with computational effort within one model setup (i.e. In calculating, the horizontal grid sizes of the ORC and OCC are chosen to be $\Delta x \simeq 19.25$ km ; $\Delta y \simeq 9.17$ km and $\Delta x \leq 55$ km ; $\Delta y \leq 45$ km respectively).

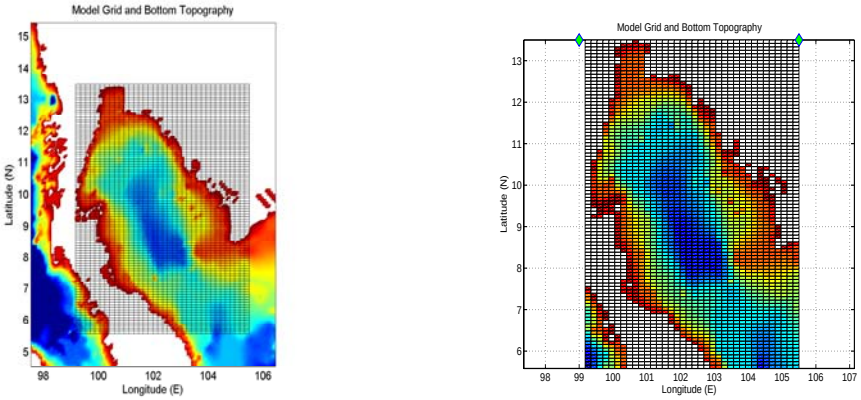

(a) (b)

Figure 6: The ORC model grid and the bottom topograph (a) used for the simulations in the GoT (m) and (b) a magnified view of the specific region.

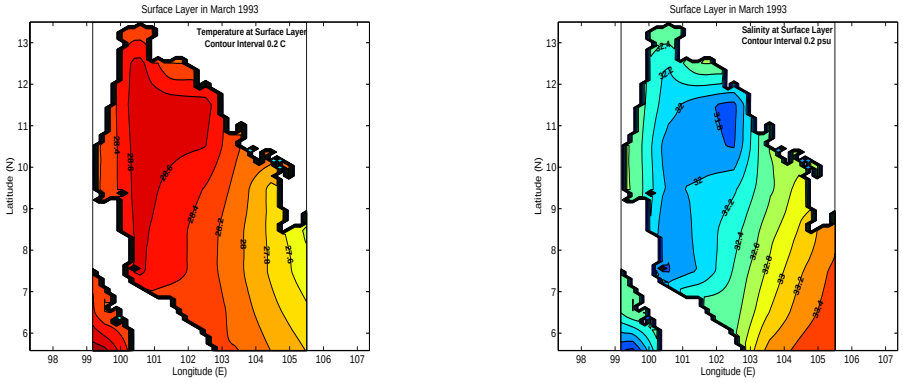

(a) (b)

Figure 7: The Initial Data of (a) Temperature (°C) and (b) Salinity (psu) at the sea surface layer in March, 1993.

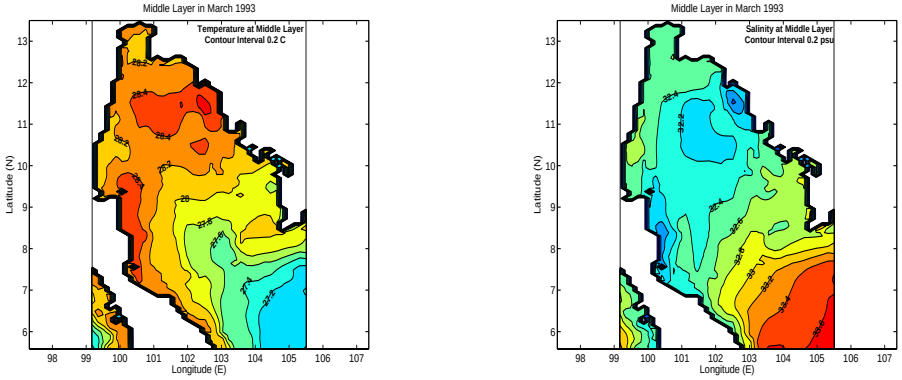

(a) (b)

Figure 8: The Initial Data of (a) Temperature (°C) and (b) Salinity (psu) in the middle layer in March, 1993.

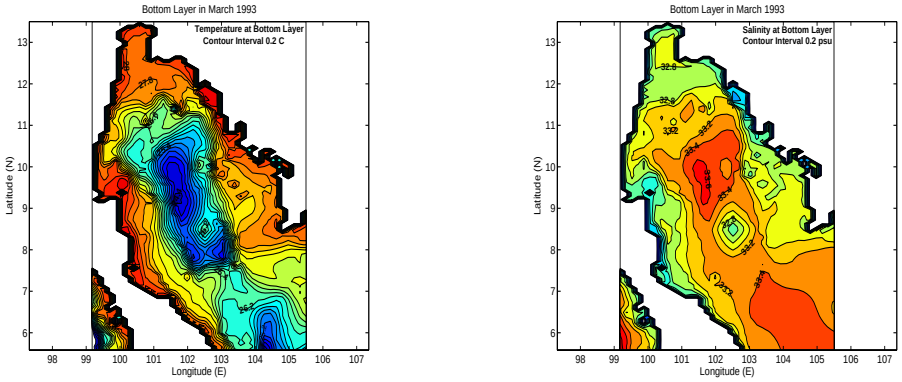

(a) (b)

Figure 9: The Initial Data of (a) Temperature (°C) and (b) Salinity (psu) at the bottom layer in March, 1993.

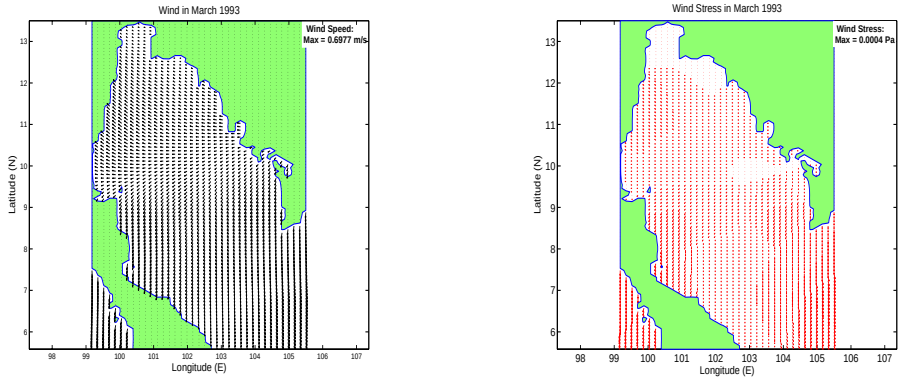

(a) (b)

Figure 10: The Initial Data of (a) Wind ($m\ s^{-1}$) at 10 m and (b) Surface wind stress (Pa) in March, 1993.

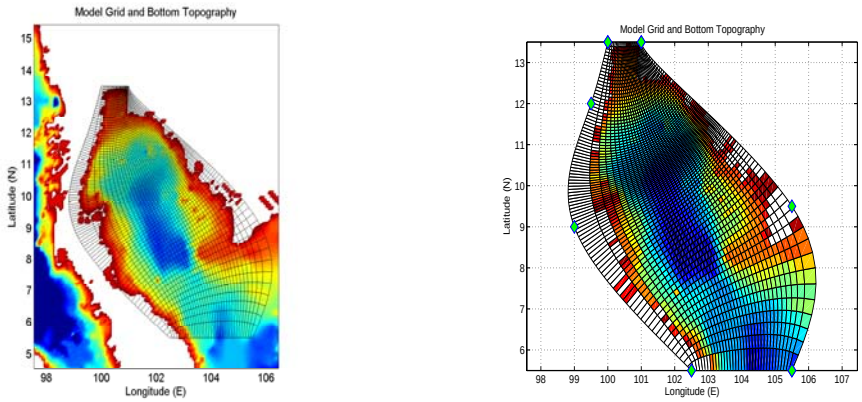

(a) (b)

Figure 11: The OCC model grid and the bottom topograph (a) used for the simulations in the Gulf of Thailand (m) and (b) a magnified view of the specific region.

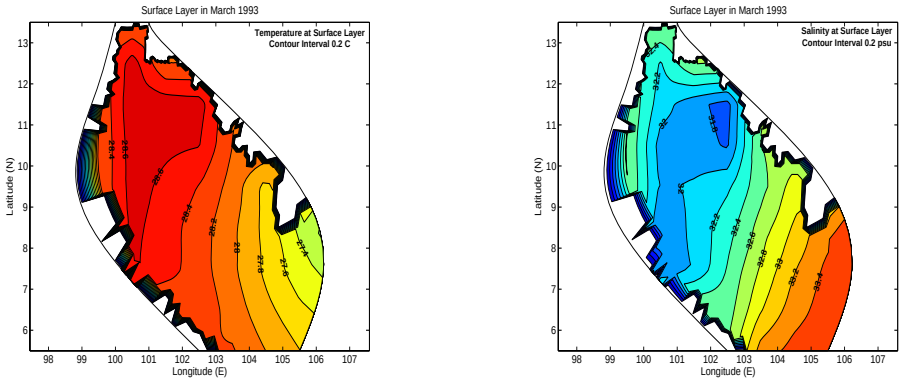

(a) (b)

Figure 12: The Initial Data of (a) Temperature (°C) and (b) Salinity (psu) at the sea surface layer in March, 1993.

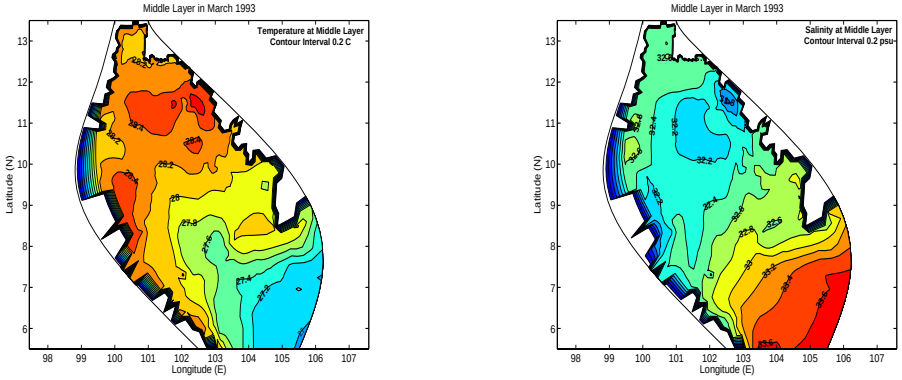

(a) (b)

Figure 13: The Initial Data of (a) Temperature (°C) and (b) Salinity (psu) in the middle layer in March, 1993.

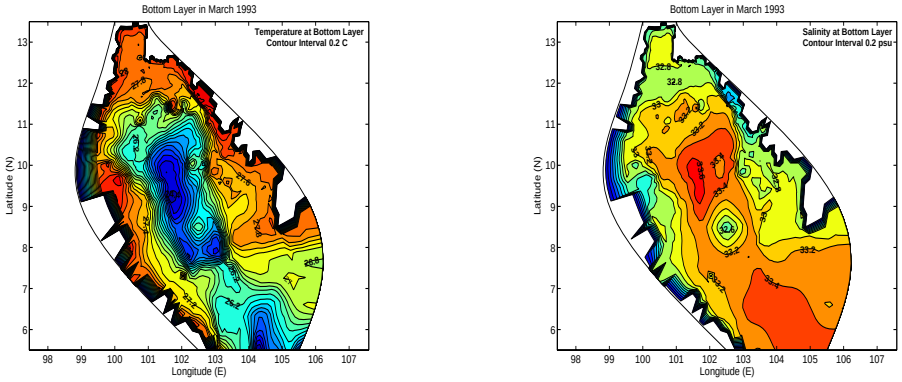

(a) (b)

Figure 14: The Initial Data of (a) Temperature (°C) and (b) Salinity (psu) at the bottom layer in March, 1993.

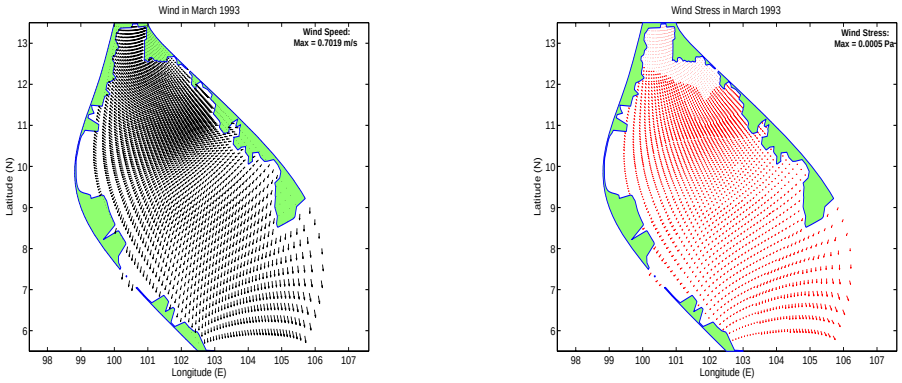

(a) (b)

Figure 15: The Initial Data of (a) Wind ($m\ s^{-1}$) at 10 m and (b) Surface wind stress (Pa) in March, 1993.

The wind stress is calculated directly from surface wind velocity, $\mathbf{V}_a$, by using the quadratic law

$$(\tau_{0x}, \tau_{0y}) \quad = \quad \rho_a C_D |\mathbf{V}_a|(U_a, V_a) \tag{3.1}$$

where ρ_a is the sea level air density ($kg \cdot m^{-3}$) and C_D is the drag coefficient which varies from about 0.001 to 0.0025 depending on the wind speed itself suggested by Matthias and Godfrey (1994). The CD is calculated by

$$C_D \quad = \quad Min\{0.001 + 0.00007|\mathbf{V}_a|, 0.0025\}. \tag{3.2}$$

For the first model run, the wind velocities, $\mathbf{V}_a$, are taken from ECMWF climatological monthly mean wind velocity measured at 10 m above the sea surface. At the bottom of the Gulf, the normal gradients of $Temperature$ and $Salinity$ are zero, so that there are no advective and diffusive heat and salt fluxes across the boundary. Nevertheless there is an additional bottom friction force depending on the velocity adjacent to the boundary. The bottom stress described by matching the velocities with the logarithm law of the wall is

$$(\tau_{bx}, \tau_{by}) \quad = \quad \rho_a C_z |\mathbf{V}_b|(U_{bx}, V_{by}) \tag{3.3}$$

where $\mathbf{V}_b$ is the nearest bottom velocity. A coefficient of bottom friction, C_z, will increase in value when wave effects are presented. This value can be obtained from the following equation by Mellor (2004)[18]

$$C_z \quad = \quad Max\Big\{\frac{\kappa^2}{\Big[\ln\frac{(1+\sigma_{kb-1})H}{z_0}\Big]^2}, 0.0025\Big\}, \tag{3.4}$$

where κ is the von Kármán constant; kb is the total number of sigma vertical level, and z_0 is the bottom roughness parameter. In this paper κ is taken to be 0.4, while $z_0 = 0.01\ m$ is used by Weatherly and Martin (1978).

3.2 Results and Discussion

For the model run, the program has the following steps: generate the horizontal and vertical grid; read the bottom topography and interpolate to the grid; read the wind velocity, temperature and salinity and interpolate to the grid; write grid and initial conditions for model; write the initial data and use it to drive the POM2k; and last of all, write the results for the Matlab plot. In calculating, the horizontal grid sizes of the ORC and OCC model are chosen to be $\Delta x \simeq 19.25\ km$; $\Delta y \simeq 9.17\ km$ and $\Delta x \leq 55\ km$; $\Delta y \leq 45\ km$, respectively. The time step sizes of the both model are chosen as $\Delta t_i = 900\ s$ in the internal mode, $\Delta t_e = 30\ s$ in the external mode and α= 0.2250 (weak filter) for the development and stability process. In this paper, we consider the circulation at the sea surface in the external mode. The time step sizes are chosen as $\Delta t_i = 900\ s$ in the internal mode, $\Delta t_e = 30\ s$ in

the external mode and $\alpha = 0.2250$ (weak filter) for the development and stability process. For typical coastal ocean conditions, the ratio of the time steps, $\Delta t_i/\Delta t_e$ = dti/dte = isplit, is often a factor of 30-80 or larger. For more information on the sensitivity of POM to time steps, see e.g. Mellor (2004). After input the initial data of the bottom topography, temperature, salinity and wind stress by using the interpolation of the monthly mean, the POM2k model is driven for one year by using the initial data of the sample month (i.e. March) so that we can consider the affect of the bottom topography, temperature, salinity and wind stress to the simulation of the ORC and OCC circulation in the GoT. The sample results after driving the model for the periods on March 29-31, 1994. The OCC circulation is setup the initial data as ORC circulation which the comparison of velocity vector fields between the ORC circulation and OCC circulation in the GoT near coastal has been shown in Figure 16-18, respectively.

From the sample results after driving the model, we find many effects of the simulation in the GoT (i.e. the effects of the horizontal grids, vertical resolutions, smoothing the bottom topography and the σ-distribution). In this study, we concentrate on the effects of the OCC grids and compare the result with the ORC grids (i.e. we set the resolution grid points of the ORC grids as same as the number of the OCC grids : 37×97 in longitude (E), latitude (N) and 10 vertical levels respectively). The error growth and distribution are studied by using the horizontal curvilinear grids and the uniformly distributed horizontal rectangular grids. After 30-40 days of integration the model has been spun up, and the error velocity fields reach a statistically stable state after that (i.e. In the model setup, we check by the variation of the volume-averaged mean kinetic energy). The maximum magnitude of the error velocities about 0.01 $m\ s^{-1}$ at the northeast wall of the GoT submarine canyon are interesting for the case study. The vector fields of the averaged velocity induced by the pressure gradient error (PGE) are presented for day 363-365 using OCC grids and compared with ORC grids shown in Table 1.

Grid systems	The maximum magnitude of the error velocities (m/s) in March, 1994		
	March 29(day 363)	March 30(day 364)	March 31(day 365)
1. OCC Grids	0.1292	0.1288	0.1283
2. ORC Grids	0.1124	0.1100	0.1077

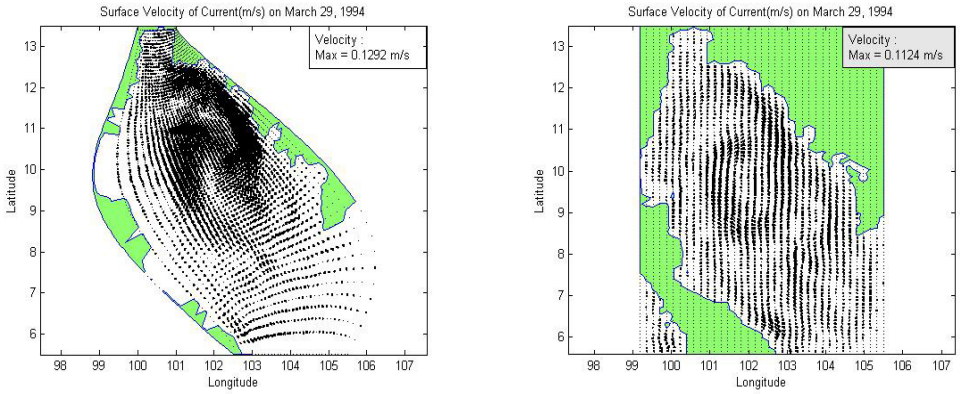

(a) (b)

Figure 16: The distribution of the velocity induced by the PGE using (a) the OCC grids and (b) the ORG grids on day 363.

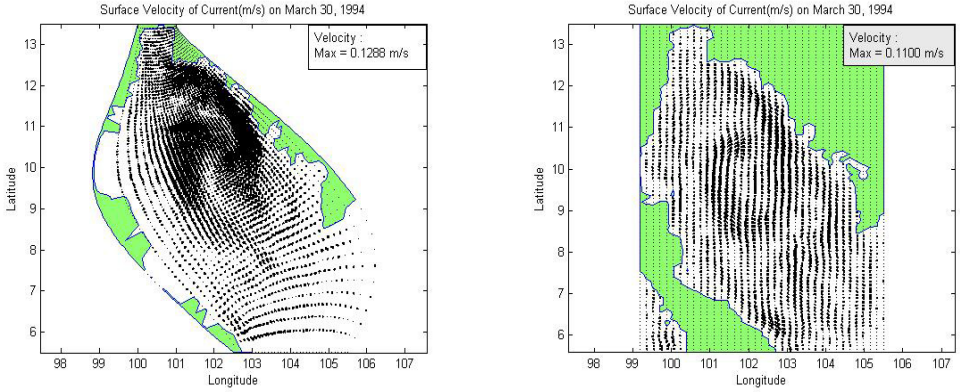

(a) (b)

Figure 17: The distribution of the velocity induced by the PGE using (a) the OCC grids and (b) the ORG grids on day 364.

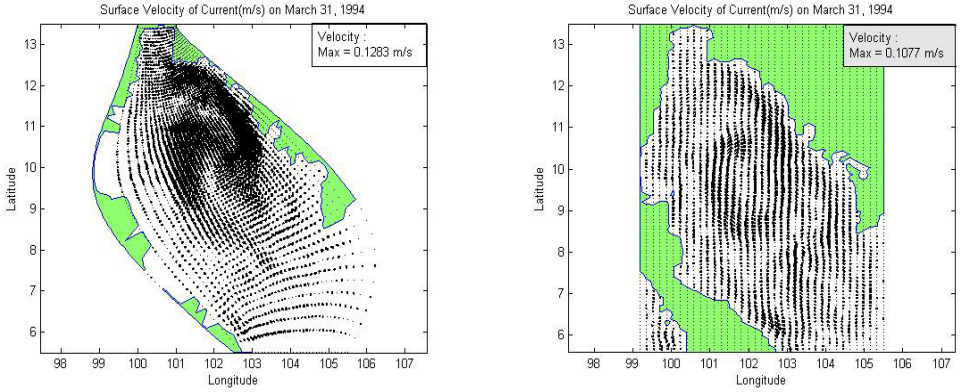

(a) (b)

Figure 18: The distribution of the velocity induced by the PGE using (a) the OCC grids and (b) the ORG grids on day 365.

4 Conclusions

The simulated currents at the surface level induced by wind from observation indicate that the actual flows are produced directly by the wind forcing. The wind induced circulation inside the Gulf is characterized by the migration of water from the southeast to the north of the Gulf as an effect of the wind forcing. The three-dimensional circulation model discussed in this paper is well tested and operational, as well. The use of the OCC system has made possible high resolution where it is required without paying the penalty imposed by unnecessary high resolution in other parts of the region. By virtue of providing reliable dynamic and thermodynamic properties, it is believed that the circulation model will be useful for simulating the circulation of estuarine and coastal ocean regions. From the comparison of the OCC circulation and ORC circulation, we find that the OCC circulation is available for the GoT region because the GoT has two bending of topography in the coastlines, especially, the horizontal OCC grid system. In addition, the presented coastal ocean σ-coordinate model (POM) of the GoT region can be used with confidence regarding horizontal PGE and the advantage of the model can describe the circulation in the OCC system near shoreline for many years later.

5 Acknowledgements

The authors would like to acknowledge the Commission on Higher Education for a financial support of Mr.Worachat Wannawong under the Strategic Scholarships Fellowships Frontier Research Networks (CHE-PhD-THA-NEU) in 2007. Finally, I would like to thank the oceanic mathematical modeling research group and rocks cluster distribution in the computer laboratory of the mathematics department, faculty of science, King Mongkuts University of Technology Thonburi for the advanced research.

References

[1] Arakawa, A., and Lamb, V.R. (1977). Computational Design of the Basic Dynamical Processes of the UCLA General Circulation Model, *Methods in Computational Physics* 17, edited by Chang J., Academic, San Diego, Calif., 173–265.

[2] Aschariyaphotha, N., Wongwises, P. and Humphries, U.W. (2004). Interpolation of Climatological Data to Numerical Ocean Modeling for the Gulf of Thailand, *Proceeding of the Joint International Conference on Sustainable Energy and Environment* 7-001, 784–789.

[3] Blumberg, A.F., and Herring, H.J. (1986). Circulation Modelling Using Orthogonal Curvilinear Coordinates, *Proceeding of the 18th International Liege Colloquim on Ocean Hydrodynamics.*

[4] Blumberg, A.F., and Mellor, G.L. (1987). A description of a threedimensional coastal ocean circulation model. Three-Dimensional Coastal Ocean Models N. Heaps, Ed., Coastal and Estuarine Sci., *Amer. Geophys. Union.* 4, 1–16.

[5] Cox, M.D. (1984). A primitive equation, three-dimensional model of the ocean, *GFDL Ocean Group Tech. Rep. No. 1*, GFDL, Princeton, NJ, 144pp.

[6] Haidvogel, D.B., Beckman, A. and Hedstrom, K.S. (1991). Dynamical simulations of filament formation and evolution in the coastal transition zone, *J. Geophys. Res.* 96, 15, 01715, 040.

[7] Ives, D.C., and Zacharias, R.M. (1987). Conformal mapping and Orthogonal grid generation, *AIAA/SAE/ASME/ASEE 23rd Joint Propulsion Conference Paper No. 87-2057*, San Diego, California.

[8] Levitus, S., and Boyer, T. (1994)a. World Ocean Atlas 1994, Temperature, *NOAA Atlas NESDIS* 4, 117pp.

[9] Levitus, S., Burgett, R. and Boyer, T. (1994)b. World Ocean Atlas 1994, Salinity, *NOAA Atlas NESDIS* 3, 99pp.

[10] Madec, G., and Imbard, M. (1996). A global ocean mesh to overcome the North Pole singularity, *Climate Dyn* 12, 381388.

[11] Mathias, T., and Godfrey, J.S. (1994). Regional Oceanography: An Introduction, *Pergamon*, Australia.

[12] Mellor, G.L. (2004). Users Guide for a Three-Dimensional, Primitive Equation, *Numerical Ocean Model*, Princeton University.

[13] Murray, R.J. (1996). Explicit generation of orthogonal grids for ocean models, *J. Comput. Phys.* 126, 251273.

[14] Smagorinsky, J. (1963). Ceneral circulation experiments with the primitive equations, I. The basic experiment, *Mon. Weather Rev.* 91, 99164.

[15] Smith, R.D., Kortas, S. and Meltz, B. (1995). Curvilinear coordinates for global ocean models, *Tech. Note LA-UR-95-1146, Los Alamos National Laboratory*, 38pp.

[16] UNESCO. (1981). Tenth Rep. of the Joint Panel on Oceanographic Tables and Standards, *UNESCO Tech. Pap. In Marine Science*.

[17] U.S. Naval Oceanographic Office and the U.S. Naval Ocean Research and Development Activity. (1983). DBDB5 (Digital Bathymetric Data Base-5 Minute Grid), *U.S.N.O.O., Bay St. Louis*.

[18] Weatherly, G., and Martin, P.J. (1978). On the Structure and Dynamics of the Ocean Bottom Boundary Layer, *Journal of Physical Oceanography* 8, 557570.

[19] Wilkin, J.L. (1987). A computer program for generating two-dimensional orthogonal curvilinear coordinate grids, *Unpublished manuscript*, 12pp.

[20] Wannawong, W., Humphries, U.W. and Luadsong, A. (2006). Sea surface elevation of the primitive equation oceanic model for the Gulf of Thailand, *Thai Journal of Mathematics Special Issue (Annual Meeting in Mathematics)*, 83100.

(Received 25 May 2007)

W. Wannawong, U. Humphries and A. Luadsong
Department of Mathematics
Faculty of Science
King Mongkut's University of Technology Thonburi
Bangkok 10140, THAILAND.
e-mail: worachataj@yahoo.com